Biochimica et Biophysica Acta 1800 (2010) 31–39

Contents lists available at ScienceDirect

Biochimica et Biophysica Acta

journal homepage: www.elsevier.com/locate/bbagen

A novel protein found in the I bands of myofibrils is produced by alternative splicing of the *DLST* gene ☆

Sadayuki Matuda [a], Takuro Arimura [b], Akinori Kimura [b], Hiroaki Takekura [a], Shigeo Ohta [c], Kyoko Nakano [d,*]

[a] Department of Biology and Health Science, Kanoya National Institute of Fitness and Sports, Kanoya, Kagoshima 891-2393, Japan
[b] Department of Molecular Pathogenesis, Medical Research Institute, Tokyo Medical and Dental University, Bunkyo-ku, Tokyo 113-8510, Japan
[c] Department of Biochemistry and Cell Biology, Institute of Development and Aging Sciences, Graduate School of Medicine, Nippon Medical School, Kawasaki, Kanagawa 211-8533, Japan
[d] Department of Biochemistry, Kagoshima Women's Junior College, Kagoshima, Kagoshima 890-8565, Japan

ARTICLE INFO

Article history:
Received 25 June 2009
Received in revised form 17 September 2009
Accepted 2 October 2009
Available online 9 October 2009

Keywords:
Dihydrolipoamide succinyltransferase (*DLST*) gene
α-Ketoglutarate dehydrogenase complex
Alternative splicing
Myofibril-protein
Skeletal muscle
I band

ABSTRACT

Background: It is not known if the dihydrolipoamide succinyltransferase (*DLST*) gene, a mitochondrial protein, undergoes alternative splicing. We identified an uncharacterized protein reacting with an anti-DLST antibody in the I bands of myofibrils in rat skeletal muscle.
Methods: Immunocytochemical staining with an anti-DLST antibody, the purification and amino acid sequence analysis of the protein, and the isolation and sequencing of the protein's cDNA were carried out to clarify the properties of the protein and its relationship to the *DLST* gene.
Results: A pyrophosphate concentration >10 mM was necessary to extract the protein from myofibrils in the presence of salt with a higher concentration than 0.6 M, at an alkaline pH of 7.5–8.0. The protein corresponded to the amino acid sequence of the C-terminal side of DLST. The cDNAs for this protein were splicing variants of the *DLST* gene, with deletions of both exons 2 and 3, or only exon 2 or 3. These variants possessed an open reading frame from an initiation codon in exon 8 of the *DLST* gene to a termination codon in exon 15, generating a protein with a molecular weight of 30 kDa.
Conclusions: The *DLST* gene undergoes alternative splicing, generating the protein isolated from the I bands of myofibrils.
General significance: The *DLST* gene produces two different proteins with quite different functions via alternative splicing.

1. Introduction

The α-ketoglutarate dehydrogenase complex is a mitochondrial enzyme that catalyzes the oxidative decarboxylation of α-ketoglutarate to succinyl-CoA [1–4]. This complex is composed of multiple copies of three different catalytic enzymes, α-ketoglutarate dehydrogenase, dihydrolipoamide succinyltransferase (DLST), and dihydrolipoamide dehydrogenase. The self-assembly of multiple copies of DLST forms the structural core of the complex, to which multiple copies of α-ketoglutarate dehydrogenase and dihydrolipoamide dehydrogenase bind noncovalently. We previously reported the isolation and sequence of the human and rat cDNAs for DLST [5,6]. The mature DLST proteins of human and rat are constituted of 386 amino acid residues. The human and rat *DLST* genomic genes have been also isolated and sequenced [7,8]. The human and rat *DLST* genes are approximately 23 kb in size with 15 exons.

To date, DLST has been found only in mitochondria. However, our previous immunostaining study showed that the plasma membrane of skeletal muscle, in addition to the mitochondria, was positive for the staining with an anti-DLST antibody [9]. We have since investigated the staining of rat skeletal muscle and have found that this protein is present in the I bands of myofibrils in rat skeletal muscle.

In the present study, we isolated the protein that reacts with an anti-DLST antibody from myofibrils of rat skeletal muscle and determined its amino acid sequence. Furthermore, we also isolated the cDNA corresponding to this protein from a rat skeletal muscle cDNA library and determined its nucleotide sequence. We report here that the protein reacting with the anti-DLST antibody is the product of alternative splicing of the *DLST* gene. The protein was designated DLSTpdi; DLST-a protein differing in structure and function (DLSTpdi) based on the observation that the protein is coded by the *DLST* gene but differs from DLST in terms of function and structure, as described later.

2. Materials and methods

2.1. Materials

A cap site cDNA library was obtained from Nippon Gene (Toyama, Japan). Total RNA from rat skeletal muscle and the reverse transcription

☆ The sequence data in this paper have been submitted to DDBJ, EMBL and GenBank Data Libraries under the accession numbers AB504752, AB504753 and AB504754.

* Corresponding author. Tel.: +81 99 254 9191; fax: +81 99 254 5914.
E-mail address: nakano@jkajyo.ac.jp (K. Nakano).

0304-4165/$ – see front matter © 2009 Published by Elsevier B.V.
doi:10.1016/j.bbagen.2009.10.003

(RT)-polymerase chain reaction (PCR) kit were obtained from BioChain Institute Inc. (USA) and Takara Bio. Co. (Kyoto, Japan), respectively.

2.2. Immunohistochemical staining of skeletal and cardiac muscles

For the immunohistochemical analysis of rat skeletal muscle, cryosections of 10-μm thickness were prepared from rat skeletal muscle fixed in acetone. The sections were immunolabeled by immunofluorescence using anti-DLST, anti-ryanodine receptor (Sigma-Aldrich, USA), and anti-α-actinin (Sigma-Aldrich, USA) antibodies in the dilutions of ×150–×250 . For the immunostaining of skeletal and cardiac muscles of human and mouse, human and mouse (C57BL/6) tissues were fixed in 10% phosphate-buffered formalin, embedded in paraffin wax, sectioned at 5 μm. Tissue sections after deparaffinization step were incubated for 10 min with antigen liberation solution (0.01 M citrate buffer, pH6.0) at 120 °C in an autoclave, followed by cooling, and incubated for 1 h with blocking solution (10% bovine serum, 0.03% Triton-X in PBS) at room temperature. Human heart sections were incubated with primary rabbit anti-DLST (1:200) and mouse anti-α-actinin antibodies (1:200, Sigma-Aldrich, USA) overnight at 4 °C. Mouse diaphragm and heart sections were immunoreacted with primary rabbit anti-DLST and mouse anti-telethonin antibodies (1:100, BD Biosciences, USA) using Vector M.O.M. Immunodetection kit (Vector Laboratories Inc., USA) according to manufacture's instruction. The sections were washed with 0.03% Triton-X in PBS and incubated with secondary sheep anti-rabbit IgG FITC-conjugated antibody (1:200, Chemicon, Australia) and Alexa fluor 568 goat anti-mouse IgG_1 antibody (1:250, Molecular probes, USA) for 1 h at room temperature. The images were analyzed with an LSM510 laser-scanning microscope (Carl Zeiss Microscopy, Germany).

2.3. Isolation of DLSTpdi from rat skeletal muscle

All procedures were carried out at 4 °C. Rat skeletal muscle was removed from the thigh and washed with 5 mM Tris–HCl (pH 7.4) containing 0.15 M KCl and 0.1 mM EDTA (solution A). The skeletal muscle was pulverized with a razor and homogenized in 9 volumes of solution A with an Ultra-Turrax homogenizer. Triton X-100 was added to a final concentration of 1% to the homogenate, and the homogenate was stirred for 15 min. The homogenate was then filtered through coarse gauze and centrifuged at 800×*g* for 15 min. The precipitate was washed several times with solution A containing 1% Triton X-100 to remove mitochondrial DLST. The precipitate was finally recovered as myofibril.

To extract DLSTpdi from the myofibrils, we first eliminated other proteins that were bound to the myofibrils. Namely, the myofibrils were suspended in 9 volumes of 20 mM Tris–HCl (pH 7.8) containing 0.4 M NaCl and 5 mM pyrophosphate and then stirred for 20 min. The suspension was centrifuged at 12,000×*g* for 20 min, and the precipitate was recovered. This was repeated four times to remove myosin, tropomyosin, and other proteins; after the final wash the precipitate was recovered. The precipitate was then treated with 7 volumes of 20 mM Tris–HCl (pH 7.8) containing 0.6 M NaCl and 15 mM pyrophosphate and stirred for 20 min. The suspension was centrifuged at 12,000×*g* for 20 min, and the supernatant containing the majority of the PCP was recovered. The supernatant was dialyzed overnight against a 5 mM phosphate–K buffer (pH 6.5) containing 1 mM pyrophosphate and then centrifuged at 13,000×*g* for 20 min, and the supernatant was recovered.

The sample was then fractionated with ammonium sulfate. Ammonium sulfate was added to the recovered supernatant to 0.4 saturation, stirred for 30 min, and centrifuged at 13,000×*g* for 20 min. Ammonium sulfate was added to the supernatant to 0.65 saturation, stirred for 30 min, and centrifuged at 13,000×*g* for 20 min. The precipitate was dissolved in 5 mM phosphate–K buffer (pH 6.5) containing 1 mM pyrophosphate and dialyzed overnight against the same solution. The dialyzed suspension was centrifuged at 13,000×*g* for 20 min. The supernatant was recovered as a final sample purified for DLSTpdi.

2.4. Determination of amino acid sequence of DLSTpdi

The final sample of DLSTpdi was electrophoresed on sodium dodecyl sulfate-polyacrylamide gel electrophoresis (SDS-PAGE) using a 12% gel. The band corresponding to DLSTpdi was excised from the gel, and the excised slice was electrophoresed again on SDS-PAGE and electroblotted onto an immobilon P membrane. After staining with Coomassie Brilliant Blue G-250, the DLSTpdi on the membrane was treated with cyanogen bromide for the analysis of its internal amino acid sequence and subjected to the amino acid analyzer of the Procise 494 HT Protein Sequencing System.

2.5. Preparation of anti-DLST antibody

The C-terminal region of DLST, which contained the region downstream from the methionine in exon 8 of the *DLST* gene, was expressed with glutathione-S-transferase in *Escherichia coli*. Inclusion bodies containing the fusion protein were isolated and subjected to preparative SDS-PAGE. The fusion protein was eluted from the excised gel, concentrated, and dialyzed with phosphate–K buffered saline. The anti-DLST antibody was raised in a rabbit against the fusion protein.

2.6. Isolation and sequence of cDNA for rat skeletal muscle DLSTpdi

The cDNA for skeletal muscle PCP was isolated by an oligonucleotide-capping method [10] with a cap site cDNA library from rat skeletal muscle. The first PCR was performed using the forward primer 5′-caaggtacgccacagcgtatg-3′ (1RC, Nippon gene) specified in the protocol for this approach [10] and the reverse primer 5′-gttgcacgggctagaagactgg-3′ from the 3′-noncoding region in exon 15 of the rat *DLST* gene.

For the detection of the cDNA of DLSTpdi, the first PCR-product of the cap site cDNA library (fPCR-p) was amplified using the forward primer 5′-atgctgtcccggtcccgctgcgtg-3′ from exon 1 of the *DLST* gene and the reverse primer 5′-gatgccatttgctggtgatgg-3′ from exon 7 of the rat *DLST* gene.

To obtain the full-length cDNA for DLSTpdi, the fPCR-p was amplified using the specific forward primer 5′-cgctttctgccttccagaag-cat-3′ and the reverse primer 5′-cagtaggtaggcatgtgtggc-3′ from the 3′-noncoding region in exon 15 of the rat *DLST* gene. This specific forward primer for DLSTpdi was targeted to the 20 nucleotides (5′-cgctttctgccttccagaag) from the 3′ end of exon 1 and the 3 nucleotides (cat-3′) from the 5′ end of exon 4 of the rat *DLST* gene.

2.7. RT-PCR for DLSTpdi

RT-PCR was performed using total RNA from rat skeletal muscle (BioChain Institute Inc., USA) and the Prime Script RT-PCR kit (Takara Bio. Co.). Total RNA was reverse transcribed using an oligo(dT) primer. RT-PCR was performed using the specific forward primer for rat DLSTpdi (5′-cgctttctgccttccagaagcat-3′) and the reverse primers from exon 8 (5′-gcttcagctggtttggccttagc-3′) or the 3′-noncoding region (5′-cagtaggtaggcatgtgtggc-3′) in exon 15 of the rat *DLST* gene.

2.8. Real-time quantitative RT-PCR

First-strand cDNA was synthesized with the PrimeScript RT-PCR kit (Takara Bio. Co.) using total RNA from rat skeletal muscle (BioChain Institute Inc.) and oligo(dT) primers. Real-time quantitative RT-PCR using the DNA Engine Opticon2 (MJ Research, USA) was carried out according to the principle described by Wu et al. [11]. The measurements were repeated three times, and the relative-quantitative amount was calculated by comparing the amount of mRNA of DLSTpdi or variant to the DLST, which was determined by the equation $2^{-C(t)\text{DLSTpdi or variant}-C(t)\text{DLST}}$. The real-time PCR products of DLST mRNA contain the mRNAs of DLSTpdi and the

variant. Therefore, the final result was expressed as a relative amount by comparing the relative-quantitative amount of DLSTpdi or variant to the value obtained by the equation [1.0—relative-quantitative amount of DLSTpdi and variant]. Primers and probes, which had been designed with the Primer Express software program (Applied Biosystems, USA), were as follows: the DLSTpdi forward primer, 5′-gctttctgccttccagaagcat-3′ (the DLSTpdi-specific primer); DLST forward primer, 5′-cattaacaacagtagcgtcttcagtg-3′ (exon 4); the forward primer for a variant that lacks only exon 3, a variant of DLSTpdi, 5′-agacgttccctgcctgcat-3′ (the variant-specific primer); a reverse primer for DLSTpdi, DLST and variant, 5′-gggtctggactgtaat-cacatcatt-3′; TaqMan probe for DLSTpdi, DLST and variant, 5′-cgcttcttccaaaccacggcagtg-3′. The specific forward primer for the variant that lacks only exon 3 was targeted to the 16 nucleotides (5′-agacgttccctgcctg) from the 3′ end of exon 2 and the 3 nucleotides (cat-3′) from the 5′ end of exon 4 of the rat *DLST* gene.

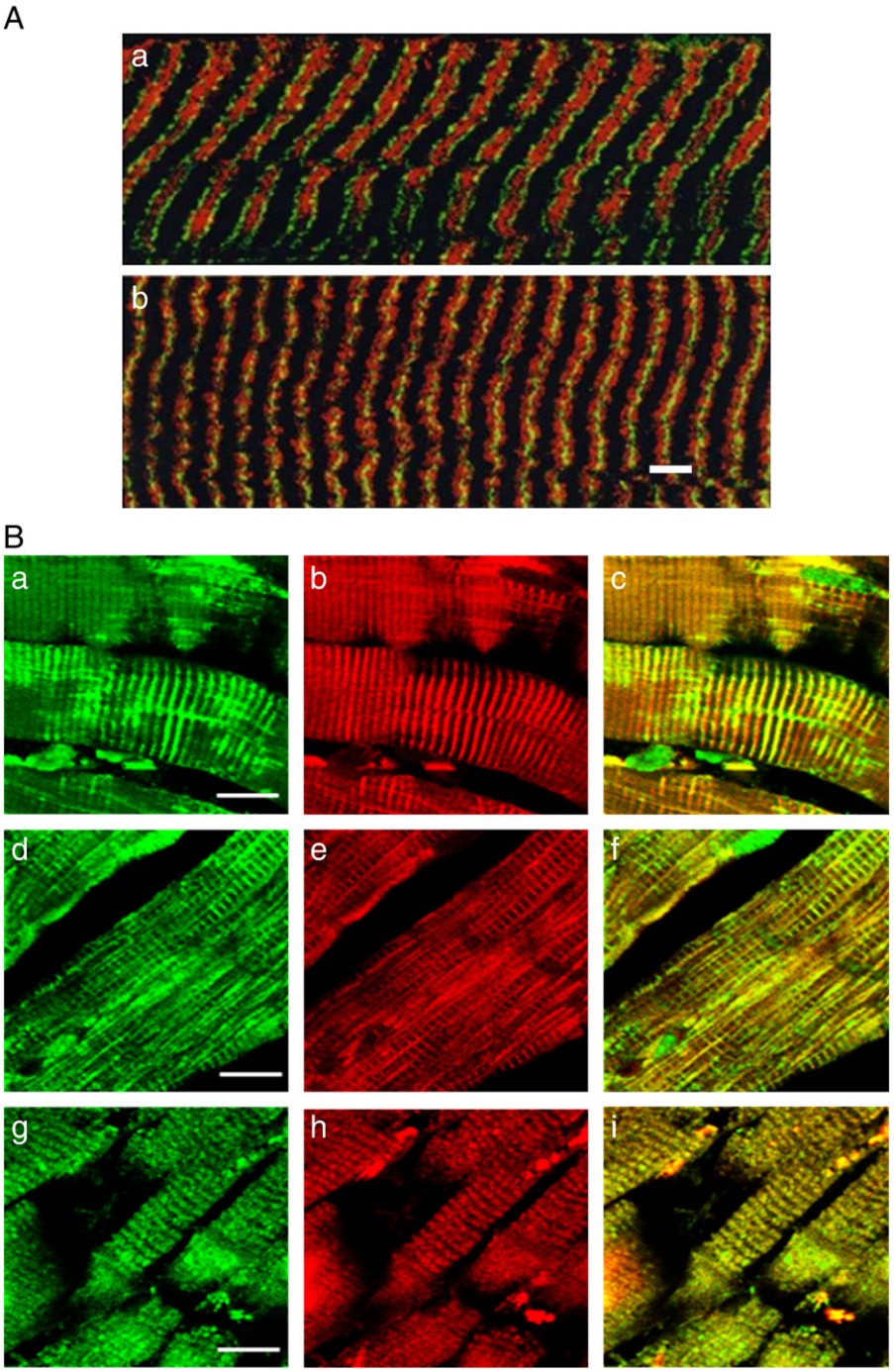

Fig. 1. Immunostaining of striated muscles with the anti-DLST antibody. (A) Immunocytochemical staining of rat skeletal muscle. (a) Double-staining of skeletal muscle with anti-DLST (red) and anti-ryanodine receptor (green) antibodies. (b) Double-staining of skeletal muscle with the anti-DLST (red) and anti-α-actinin (green) antibodies. Scale bar represents 2 μm. (B) Immunohistochemical staining of mouse diaphragm muscle (a–c), mouse heart ventricular muscle (d–f), and human heart ventricular muscle (g–i). Tissues were double-stained by anti-DLST (green) (a, d, g) with anti-Tcap (red) (b, e) or anti-α-actinin (red) (h). Merged images are also shown (c, f, i). Scale bars represent 10 μm.

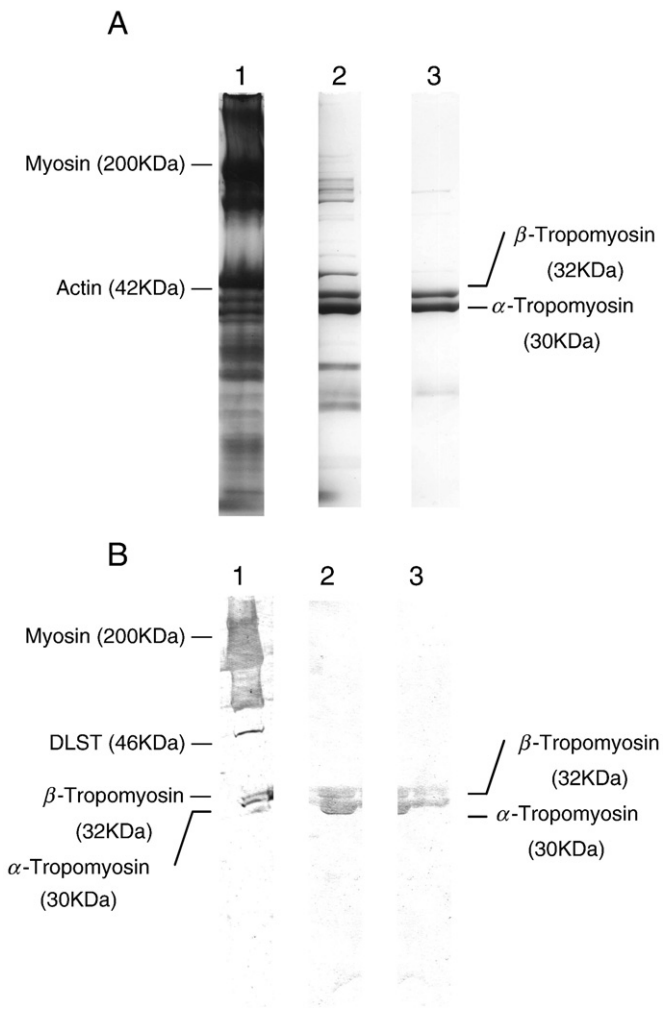

Fig. 2. SDS-PAGE and Western blotting analysis of the extract from myofibrils without pyrophosphate. (A) SDS-PAGE; (B) Western blotting analysis with anti-DLST antibody. Lane 1, final myofibrils prepared from rat skeletal muscle as described in Materials and methods. Lanes 2 and 3, myofibrils were washed several times with 20 mM Tris–HCl (pH 7.8) containing 0.4 M NaCl, and the centrifugal precipitate after the washing was treated with 20 mM Tris–HCl (pH 7.8) containing 0.6 M NaCl in the absence of pyrophosphate. After centrifugation, the supernatant was recovered and dialyzed against 5 mM phosphate buffer (pH 6.5). After dialysis and centrifugation, the supernatant was subjected to SDS-PAGE and Western blotting analysis (lane 2). Ammonium sulfate was added to the supernatant, and a fraction of 0.4–0.65 saturation was recovered. The fraction was dissolved in 5 mM phosphate buffer (pH 6.5), dialyzed against 5 mM phosphate buffer (pH 6.5), and analyzed by SDS-PAGE and Western blotting analysis (lane 3).

2.9. Conditions for PCR

PCR was amplified for 35–40 cycles under the following conditions: 95 °C for 20 s, 60 °C for 20 s, and 72 °C for 20 s. RT-PCR was amplified for 35–50 cycles under 95 °C for 30 s, 55 °C for 30 s, and 72 °C for 60 s. The conditions of real time-quantitative PCR comprised an initial denaturation step at 95 °C for 15 min, and 50 cycles at 94 °C for 15 s and 60 °C for 1 min. The nucleotide sequences of the PCR products were determined using the ABI 310 automated sequencer (Applied Biosystems).

3. Results

3.1. Immunocytochemical staining of rat skeletal muscle with anti-DLST antibody

We previously reported the immunocytochemical staining of rat skeletal muscle in paraffin sections using an antibody against purified

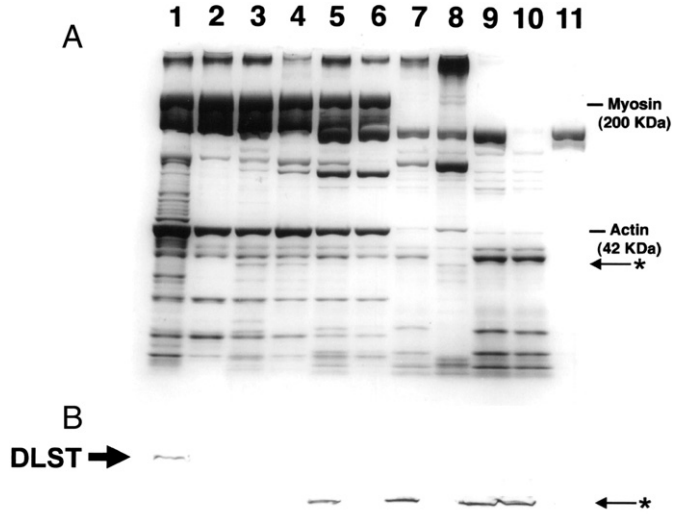

Fig. 3. SDS-PAGE and Western blotting analysis of each step from the purification of DLSTpdi in the presence of pyrophosphate. (A) SDS-PAGE; (B) Western blotting analysis of the SDS-PAGE with anti-DLST antibody. Lane 1, homogenate of rat skeletal muscle; lane 2, prepared myofibrils; lane 3, extract from rat myofibrils with 0.4 M NaCl and 5 mM pyrophosphate (pH 6.5). Lanes 4 and 5, centrifugal precipitate (lane 4) and centrifugal supernatant (lane 5) after the treatment of rat myofibrils with 0.6 M NaCl and 15 mM pyrophosphate (pH 6.5). Lanes 6 and 7, centrifugal precipitate (lane 6) and centrifugal supernatant (lane 7) after dialysis of the supernatant of lane 5 against 5 mM phosphate–K buffer (pH 6.5) containing 1 mM pyrophosphate. Lanes 8 and 9, the 0.4 saturation fraction (lane 8) and the 0.4–0.65 saturation fraction (lane 9) of the supernatant used in lane 7 with ammonium sulfate. Lanes 10 and 11, centrifugal supernatant (lane 10) and precipitate (lane 11) after dialysis of the 0.4–0.65 saturation fraction against 5 mM phosphate–K buffer (pH 6.5) containing 1 mM pyrophosphate. The small arrow with an asterisk in panel A corresponds to the small arrow with an asterisk in panel B. The large arrow indicates DLST.

DLST from the rat heart [9]. We observed staining for protein on the plasma membrane and myofibrils. In this study, frozen sections and antibody against purified recombinant DLST were subjected to double

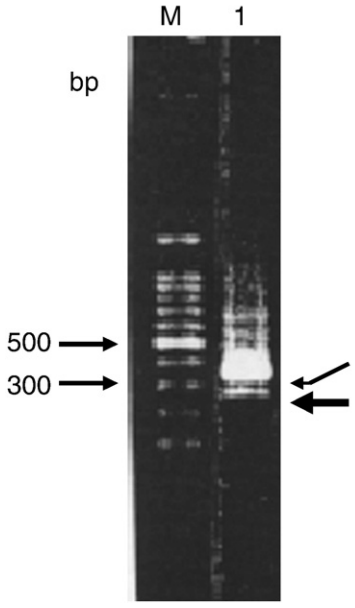

Fig. 4. Detection of DLSTpdi-cDNA. A cap site cDNA library prepared from rat skeletal muscle was used as the template. Since the nucleotide in exons 2 and 3 is about 70 bp and is short, it is difficult to separate the DLSTpdi-cDNA longer than 1000 bp from the DLST-cDNA on the agarose gel. Therefore, PCR amplification was performed in the short length of the nucleotide to detect the DLSTpdi-cDNA. The experimental procedure was described in Materials and methods. M, molecular marker; lane 1, PCR product. A large and a small arrow on the right side indicates the cDNA for PCP and DLST, respectively.

staining by immunofluorescence using two antibodies against α-actinin and the ryanodine receptor. The α-actinin is located on the Z line [12,13], and the ryanodine receptor [14,15] is located on the sarcoplasmic reticulum, which is present on the boundary between I and A bands in mammalian skeletal muscle. The Z line is situated between the two sarcoplasmic reticula. Upon double staining with the anti-DLST and anti-ryanodine receptor antibodies, we observed that DLSTpdi was sandwiched by two ryanodine receptors (Fig. 1A, a). In double staining with the anti-DLST and anti-α-actinin antibodies, a part of the DLSTpdi was stained together with the α-actinin, but another part of the DLSTpdi was stained at a short distance from the Z line (Fig. 1A, b). These results indicate that the DLSTpdi is localized in the I bands of myofibrils.

Localization of DLSTpdi in the diaphragm muscle from mouse was also examined. Immunofluorescence analyses revealed that DLSTpdi was co-distributed with telethonin, indicating that DLSTpdi is localized at the Z lines in the skeletal muscle (Fig. 1B, a–c). We also investigated the localization of DLSTpdi in the ventricular muscles of heart tissues from mouse and human. Similar localization of PCP compared to diaphragm muscle from mouse was observed at Z lines in the ventricular muscles of heart from both mouse and human (Fig. 1B, d–f and g–i, respectively). Thus, DLSTpdi appeared to localize at the I bands of skeletal and cardiac muscle cells.

3.2. Isolation of DLSTpdi from myofibrils of rat skeletal muscle

3.2.1. Isolation of DLSTpdi in the absence of pyrophosphate

Since DLSTpdi was localized in the I bands of the myofibrils, we initially isolated myofibrils from rat skeletal muscle and then isolated DLSTpdi from the prepared myofibrils. To isolate DLSTpdi from the prepared myofibrils, we attempted to purify the DLSTpdi in the absence of pyrophosphate. However, this resulted in the diffusion of DLSTpdi into the fractions of myosin, α-actinin, and tropomyosin, and it was not recovered efficiently. In Fig. 2, we show an example in which tropomyosin and DLSTpdi were recovered together with the two broad bands of the α- and β-subunits of tropomyosin (Fig. 2, lanes 2 and 3). In addition, even when the myofibrils were electrophoresed on SDS-PAGE, DLSTpdi of various molecular sizes was observed on the gel, showing no main band (Fig. 2, lane 1).

3.2.2. Isolation of DLSTpdi in the presence of pyrophosphate

Several attempts in the isolation of the DLSTpdi were tried to address the faults of the diffusion of the DLSTpdi in various molecular sizes and the low efficient recovery, and it was found that the addition of pyrophosphate during the isolation of DLSTpdi from myofibrils resolved these issues. Purification of DLSTpdi in the presence of pyrophosphate yielded a single sharp band of 30 kDa in the Western blotting analysis, showing that there was no reaction of tropomyosin with the anti-DLST antibody (Fig. 3).

Therefore, it was concluded that the protein reacting with the anti-DLST antibody in the I band of skeletal muscle was this 30-kDa protein. In addition, it should be noted that the protein was not extracted from myofibrils in the presence of 0.4 M NaCl and 5 mM pyrophosphate (Fig. 3, lane 3) but was extracted in the presence of 0.6 M NaCl and 10 mM pyrophosphate (Fig. 3, lane 5), suggesting that the protein firmly binds to the myofibrils. It is likely that the protein possesses the ability to bind to other proteins. Even electrophoresis with SDS-PAGE did not dissociate this binding and the pyrophosphate may decrease the protein binding ability of DLSTpdi via an unknown mechanism.

Although we could not purify the DLSTpdi to single molecule, this purification method was more efficient than the other methods we tried. It is difficult to explain why the pyrophosphate decreased the diffusion of DLSTpdi. The effect of pyrophosphate on the extraction of DLSTpdi from the myofibrils was observed only at an alkaline pH of 7.5–8.0. However, in extractions with pyrophosphate at an acidic pH, the DLSTpdi again diffused into the myosin, α-actinin, and

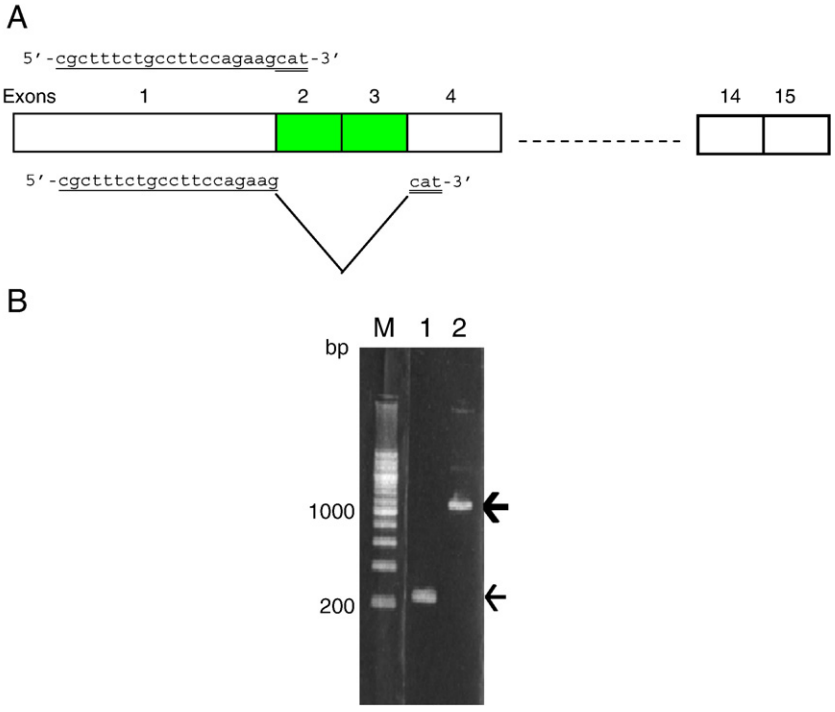

Fig. 5. Design of specific primer for DLSTpdi-cDNA and PCR amplification. A cap site cDNA library prepared from rat skeletal muscle was used as the template. The detailed experimental procedure was described in Materials and methods. (A) Scheme of the specific primer for cDNA of rat DLSTpdi. Three bases in exon 4 were used for the specific detection of cDNA for DLSTpdi. A single underline and a double underline indicate the nucleotide sequence of the 3′-side of exon 1 and of the 5′-side of exon 4, respectively. The colored boxes indicate the alternatively spliced exons. (B) PCR amplification with the specific primer for DLSTpdi. M, molecular marker; lane 1, PCR product with the specific upstream primer and the downstream primer in exon 7 (small arrow). Lane 2, PCR product with the specific upstream primer and the downstream primer in the 3′-noncoding region of exon 15 (large arrow).

```
                                                                    ATG
CTGTCCCGGTCCCGCTGCGTGTCCCGGGCGTTCAGCCGCTCGCTTTCTGCCTTCCAGAAGCAT
TAACAACAGTAGCGTCTTCAGTGTTCGCTTCTTCCAAACCACGGCAGTGTGCAAGAATGATGT
GATTACAGTCCAGACCCCAGCGTTTGCAGAGTCTGTCACAGAGGGAGATGTCAGGTGGGAGA
AAGCTGTTGGAGATGCAGTTGCAGAAGATGAAGTGGTGTGTGAGATTGAGACAGACAAGACTT
CTGTGCAGGTTCCATCACCAGCAAATGGCATCATTGAAGCTCTTTTGGTACCCGATGGGGGCA
AAGTTGAAGGAGGAACTCCTCTATTCACACTCAGGAAAACCGGTGCTGCTCCTGCTAAGGCCA
AACCAGCTGAAGCCCCTGCTACAGCCCACAAAGCAGCGCCTGAAGCACCGGCGGCCCCTCC
                                        M  P  P  V  P  S  P  S  Q  P
TCCTCCTGTAGCACCAGTGCCCACTCAG ATG CCA CCT GTG CCC TCA CCC TCA CAA CCT
  P  S  S  K  P  V  S  A  I  K  P  T  A  A  P  P  L  A
CCT TCT AGC AAA CCA GTG TCT GCA ATA AAA CCC ACT GCT GCC CCT CCA CTG GCT
  E  A  G  A  A  K  G  L  R  S  E  H  R  E  K  M  N  R
GAG GCG GGA GCT GCT AAA GGC CTG CGC TCA GAA CAT CGG GAA AAG ATG AAC AGG
  M  R  Q  R  I  A  Q  R  L  K  E  A  Q  N  T  C  A  M
ATG CGG CAG CGC ATC GCC CAG CGT CTG AAG GAA GCC CAG AAC ACC TGC GCA ATG
  L  T  T  F  N  E  V  D  M  S  N  I  Q  E  M  R  A  R
CTG ACG ACG TTC AAT GAG GTT GAC ATG AGT AAC ATA CAA GAG ATG AGA GCT CGG
  H  K  D  A  F  L  K  K  H  N  L  K  L  G  F  M  S  A
CAC AAA GAT GCT TTC CTG AAA AAA CAT AAC CTG AAA TTA GGC TTC ATG TCG GCA
  F  V  K  A  S  A  F  A  L  Q  E  Q  P  V  V  N  A  V
TTT GTG AAG GCC TCA GCA TTC GCC TTG CAG GAG CAG CCT GTA GTA AAC GCA GTG
  I  D  D  A  T  K  E  V  V  Y  R  D  Y  I  D  I  S  V
ATT GAT GAC GCA ACC AAG GAG GTG GTG TAC AGA GAT TAT ATT GAC ATC AGT GTC
  A  V  A  T  P  R  G  L  V  V  P  V  I  R  N  V  E  T
GCA GTT GCT ACC CCA AGG GGT CTC GTG GTT CCT GTC ATC AGG AAT GTG GAA ACT
  M  N  Y  A  D  I  E  R  T  I  N  E  L  G  E  K  A  R
ATG AAT TAT GCA GAT ATT GAA CGG ACC ATT AAT GAA CTA GGA GAG AAG GCC CGG
  K  N  E  L  A  I  E  D  M  D  G  G  T  F  T  I  S  N
AAG AAT GAA CTT GCC ATC GAA GAC ATG GAT GGG GGC ACC TTC ACC ATC AGC AAT
  G  G  V  F  G  S  L  F  G  T  P  I  I  N  P  P  Q  S
GGA GGA GTT TTC GGC TCA CTT TTC GGA ACA CCC ATT ATC AAC CCG CCT CAG TCT
  A  I  L  G  M  H  G  I  F  D  R  P  V  A  V  G  G  K
GCC ATT CTG GGC ATG CAT GGC ATC TTC GAC AGG CCT GTG GCT GTG GGG GGC AAG
  V  E  V  R  P  M  M  Y  V  A  L  T  Y  D  H  R  L  I
GTG GAA GTC CGA CCT ATG ATG TAT GTA GCC CTG ACC TAC GAC CAC CGG CTG ATT
  D  G  R  E  A  V  T  F  L  R  K  I  K  A  A  V  E  D
GAT GGC AGA GAG GCT GTG ACT TTC CTC CGA AAA ATC AAG GCA GCA GTA GAA GAT
  P  A  V  L  L  L  D  L  ***
CCA GCA GTC CTC CTC CTA GAC CTT TAG GAGGAAGCCACACATGCC
```

Fig. 6. Nucleotide sequence of DLSTpdi-cDNA from rat skeletal muscle. This nucleotide sequence was obtained with a combination of the short cDNA of DLSTpdi in Fig. 4 and of the cDNA for DLSTpdi isolated from the cap site cDNA library of rat skeletal muscle by PCR amplification using the specific primer for DLSTpdi and the reverse primer for the 3′-noncoding region of exon 15. The amino acid sequences underlined with the solid lines coincide with the amino acid sequences determined by the amino acid sequence analysis of DLSTpdi. The asterisks indicate the stop codon.

tropomyosin fractions. It is possible that at the alkaline pH the pyrophosphate weakens the protein binding ability of DLSTpdi.

3.3. Determination of amino acid sequence of DLSTpdi

To confirm whether the DLSTpdi was translated from the *DLST* gene, we analyzed the amino acid sequence of DLSTpdi. We initially attempted to determine the amino acid sequence of the N-terminal side of DLSTpdi. However, we could not detect the amino acid sequence of this area, which suggested that the N-terminal amino acid of DLSTpdi is modified with an unknown functional group.

We then treated SDS-PAGE-purified DLSTpdi with cyanogen bromide, which cleaves the peptide bond at the carboxyl side of methionine, and the internal amino acid sequence of DLSTpdi was analyzed. The determined amino acid sequences were RQRIAQRLK, SAFVKAS, NYADIERTI, HGIFDRP, and YVALTYDHRL. These sequences coincided with the internal amino acid sequence from the C-terminal side of rat DLST [5], suggesting that DLSTpdi consists of the C-terminal side of DLST.

3.4. cDNA for DLSTpdi

3.4.1. Detection of cDNA for DLSTpdi

As the DLSTpdi consisted of the C-terminal side of DLST, we aimed to determine if it was encoded by the *DLST* gene. To isolate

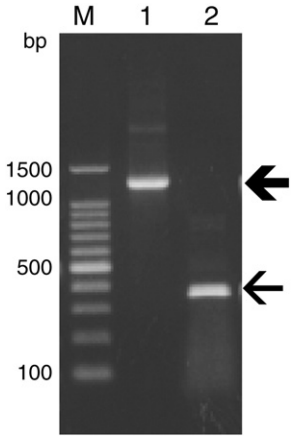

Fig. 7. Detection of rat mRNA for DLSTpdi with the specific primer. RNA was from rat skeletal muscle. The specific primer for DLSTpdi was designed as described in Fig. 5A. The detailed experimental procedure is described in Materials and methods. M, molecular DNA marker. Lanes 1 and 2 indicate the PCR-products using the specific primer (upstream) for DLSTpdi and a reverse primer in the 3′-noncoding region of exon 15 of the rat *DLST* gene (large arrow), or a reverse primer in exon 8 of the rat *DLST* gene (small arrow).

the cDNA for DLSTpdi, a cap site cDNA library from rat skeletal muscle was screened by a PCR amplification method. The PCR product consisted of two bands as observed on an agarose gel (Fig. 4, arrows), which were then analyzed for their nucleotide sequences. It was found that the major band (small arrow) corresponded to DLST-cDNA and the minor band (large arrow) predominantly contained DLST-cDNA with deletions of both exons 2 and 3; the minor band also contained a minor proportion of DLST-cDNA with deletions of either exon 2 or exon 3. These results suggest that the pre-mRNA of the *DLST* gene is alternatively spliced.

3.4.2. Design of specific primer for DLSTpdi-cDNA

Thus, the primer set used in the previous section (Fig. 4) amplified DLST-cDNAs including the alternatively spliced products. Therefore, we designed a primer that would allow for the specific amplification of the alternative splicing product (Fig. 5, panel A). Using this specific forward primer and the reverse primers in exon 7 or in the 3′-noncoding region of exon 15, the fPCR-p obtained from the cap site cDNA library from rat skeletal muscle was amplified by PCR (Fig. 5, panel B). These PCR products were analyzed for their nucleotide sequence, and the results indicated that each amplification product had deletions of both exons 2 and 3 of the *DLST* gene (Fig. 6).

3.4.3. Nucleotide sequence of DLSTpdi-cDNA

As shown in Fig. 6, the alternative splicing product contained an open reading frame (ORF) from the initiation ATG codon in exon 8 to the termination TAG codon in exon 15. The ORF of the cDNA encoded 270 amino acid residues corresponding to the C-terminal side of DLST, agreeing with the molecular size of 30 kDa for the DLSTpdi, as determined by SDS-PAGE. The nucleotide sequence surrounding the initiation codon in exon 8 resembled that of the other cDNAs [16,17]. Therefore, it was concluded that this was the cDNA for DLSTpdi, that it

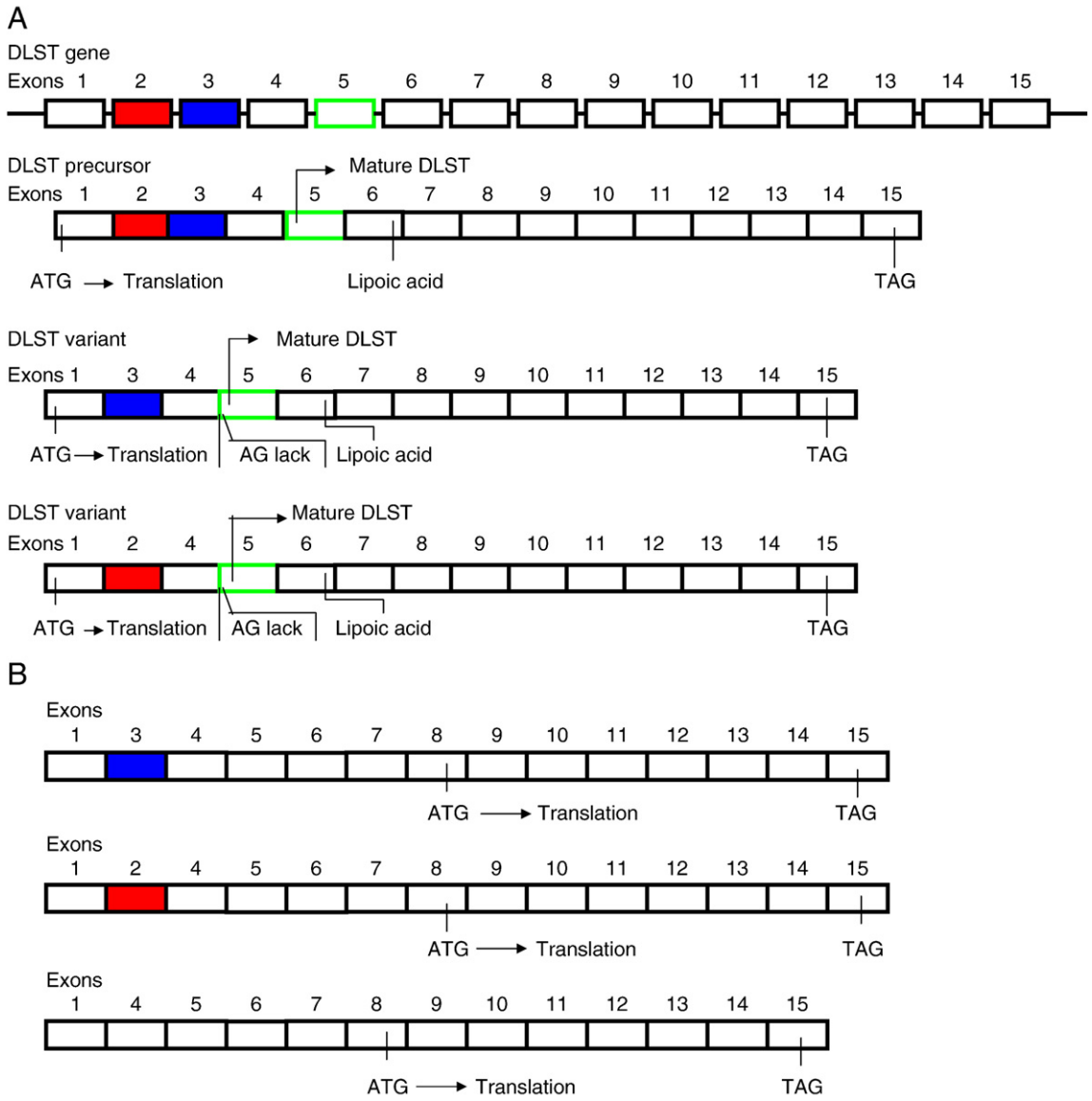

Fig. 8. Summary of alternative splicing variants of the rat *DLST* gene. (A) Structural organization of the rat *DLST* gene and its splicing variants. The variants of this type lack exon 2 or exon 3. In addition to the lack of either exon2 or exon3, this type is also missing the two AG nucleotide bases from the 5′-side of exon 5. As a result, these variants differ from each other in the amino acid sequence of the leader peptide, which is encoded by exons 1–4 and the 5′ part of exon 5. However, the leader peptides of the variants maintain the properties of the leader peptide consisting of many basic amino acids and no acidic amino acid. Lipoic acid covalently binds to the lysine in exon 6. The colored boxes indicate the alternatively spliced exons. (B) Alternative splicing variants of DLSTpdi. The variants of this type lack exon 2 or exon 3, or lack both exons 2 and 3. As a result, these variants are translated from the initiation ATG codon in exon 8 and produce the DLSTpdi protein, indicating the lack of the leader peptide for translocation into the mitochondria and of the lipoyl binding domain necessary for DLST activity. The colored boxes indicate the alternatively spliced exons.

encoded the entire DLSTpdi protein and that DLSTpdi is translated from the initiation codon in exon 8 in the alternatively spliced variant of the *DLST* gene.

3.4.4. Detection of DLSTpdi-mRNA

Using mRNA prepared from rat skeletal muscle, we performed RT-PCR to examine whether the specific primer shown in Fig. 5A is useful in detecting DLSTpdi mRNA (Fig. 7). The result demonstrated that the specific primers could detect only the specific mRNA for DLSTpdi, showing the existence of the mRNA for DLSTpdi.

3.4.5. Quantitative analysis of DLSTpdi mRNA expression

To determine the ratio of expression of the mRNAs for DLST and DLSTpdi, we performed real-time quantitative RT-PCR using RNA from rat skeletal muscle. The relative amount of DLSTpdi mRNA to DLST mRNA was 0.0034 ± 0.00066. The amount of mRNA for the variant lacking only exon 3, a variant of DLSTpdi (see Fig. 8), was also measured. The relative amount of variant mRNA to DLST mRNA was 0.0019 ± 0.00076. Therefore, the ratio of DLSTpdi mRNA to variant mRNA was calculated as approximately 1.8, indicating that the amount of DLSTpdi mRNA was more abundant than the variant.

4. Discussion

The present study has demonstrated that a novel protein, designated DLSTpdi, is expressed in the myofibrillar I bands in the striated muscles, skeletal muscle, and cardiac muscle. We have also revealed that DLSTpdi is a product derived from the alternative splicing of the *DLST* gene and that the DLSTpdi protein consists of the C-terminal side of DLST, with a molecular weight of 30 kDa.

The patterns of alternative splicing of the rat *DLST* gene are summarized in Fig. 8. The splicing forms are classified into two types; the first type (panel A) is a variant type of DLST and the second type (panel B) is a variant type of DLSTpdi. When the minor band in Fig. 4 was sequenced, it was found that these splicing variants exist. The variant with deletions of both exons 2 and 3 is the most prevalent of these splicing variants in skeletal muscle, while the other variants are less frequently observed. Thus, at present, the splicing variants of the rat *DLST* gene that were detected lack exons 2 and 3, and the two AG nucleotide bases from the 5′ of exon 5.

Prior to this study, alternative splicing of the *DLST* gene had not been well characterized. In the present study, we characterized the alternative splicing and demonstrated the presence of the I band-associated protein DLSTpdi as the products. The variant-cDNAs, lacking exons 2 and/or 3, do not possess the leader peptide for translocation into the mitochondria and the lipoyl binding domain necessary for the catalytic activity of DLST. Therefore, these variant-cDNAs cannot code for DLST and the product translated by these variant-cDNAs is transported to the I bands of myofibrils in skeletal muscle. This indicates that the variant-protein differs from DLST in function. These splicing variants of the *DLST* gene were also found in human skeletal muscle (data not shown). Furthermore, the human *DLST* gene was alternatively spliced for exon 6, which, like exons 2 and 3, is also a regulatory exon, although this splicing variant was not so prevalent. The differences in alternative splicing between rat and human may reflect species-specific alternative splicing [18].

The alternative splicing of the *DLST* gene and the alternatively translated products have not been characterized until now. It is possible that these variants would be overlooked without confirming the short deletion of about 70 bases and recognized as deletions of the 5′-nucleotide sequence. In addition, since DLSTpdi consists of the C-terminal side of DLST and the molecular size of DLSTpdi is smaller than that of DLST, DLSTpdi might be recognized as a proteolytic product of DLST. Taken together, we conclude that the lack of reports regarding the alternative splicing of the *DLST* gene may be due to the difficulty in detecting both the cDNA-variants and the associated proteins. The cDNA variants with deletions of exon 2 and/or exon 3 were also found in rat brain (data not shown). Therefore, in other tissues, DLSTpdi may possess novel functions different from its functions in myofibrils.

We have already reported that the nucleotide sequences of introns 1 and 4 are conserved among mammalian species in comparison with the other introns of the *DLST* gene [8]. In addition, it is of interest that there are no single nucleotide polymorphism (SNP) in introns 1 and 4 in comparison with the other introns of the *DLST* gene [19]. The conserved nature of introns 1 and 4 may have an important role in the alternate splicing of exons 2 and 3.

The present study suggests the possibility that the DLSTpdi is able to strongly bind to and aggregate with other proteins. This characteristic of DLSTpdi may have resulted in the varied migration of DLSTpdi in SDS-PAGE, despite the molecular weight of DLSTpdi being approximately 30 kDa. As shown in Fig. 2 (lane 1), myosin, α-actinin and tropomyosin were liable to be bound by DLSTpdi. Although DLSTpdi was released from almost all of the bound tropomyosin in the presence of pyrophosphate, it was not released from myosin and α-actinin even in the presence of this chemical. These events may suggest that the DLSTpdi strongly binds to other proteins in the I bands. Since DLSTpdi was localized in the Z lines or I bands of myofibrils, its physiological role may be to attach the myosin to the Z line through titin and actin filaments using its protein binding ability.

The Z line is composed of many kinds of proteins, and there are still unidentified proteins present in this region [20–22]. The network of proteins in the Z line is complex, and the intricate molecular architecture of the Z line is still poorly characterized. In addition, the known protein–protein interactions in the Z line appear to be insufficient in explaining the endurance against mechanical power. Proteins must exist in the Z line, which reinforce the bond between protein–protein interactions and that can bundle protein–protein interactions firmly but flexibly. DLSTpdi appears to possess such an ability. Recently, it has been reported that there is dynamic exchange of proteins between the cytosolic pool and the sarcomere, and the discovery of new proteins with unexpected properties in the Z line has been predicted [23–25].

In addition to its possible role in the structural stabilization of myofibrils in muscles, the DLSTpdi may also play a significant role in the endurance against mechanical power in the cytoskeleton of the cell since the proteins that constitute the contractile apparatus of muscle are generally found in the cell cytoskeleton [26,27]. Therefore, the physiological role and protein chemical characteristics of DLSTpdi should be resolved in the future.

In conclusion, the present study demonstrated the possibility that the *DLST* gene is multifunctional. Namely, the first function of the *DLST* gene is to produce DLST as a component of the α-ketoglutarate dehydrogenase complex involved in the tricarboxylic acid (TCA) cycle; the second function of the *DLST* gene is to produce DLSTpdi that may be involved in the structural construction of the myofibrils of muscles. Thus, the *DLST* gene produces at least two proteins with quite different functions. The multifunctional nature of the *DLST* gene may reflect the diversity of the gene. It is well known that alternative splicing produces several different proteins from one gene. It has been speculated that at least 70% of human genes undergo alternative splicing [28–31]. In almost all cases of alternative splicing, the alternatively spliced proteins possess the same or similar functions [32–36], although there is differential expression of splicing variants depending on the specific stage of development and differentiation. Furthermore, even if the intracellular localization of the splicing variant proteins differs from each other, the splicing variant proteins essentially possess the same function [37]. Therefore, it appears that the alternative splicing of the *DLST* gene, which produces two proteins with possibly quite different functions, is relatively rare in contrast to other cases of alternative splicing in which the variant proteins possess the same functions.

Acknowledgment

This research was supported in part by a grant from the Japan Science and Technology Agency and a grant for the Collaboration Research Program from Medical Research Institute, Tokyo Medical and Dental University.

References

[1] L.J. Reed, Multienzyme complexes, Acc. Chem. Res. 7 (1974) 40–46.
[2] M.S. Patel, T.E. Roche, Molecular biology and biochemistry of pyruvate dehydrogenase complex, FASEB J. 4 (1990) 3224–3233.
[3] A. Mattevi, A. de Kok, R.N. Perham, The pyruvate dehydrogenase complex, Curr. Opin. Struct. Biol. 2 (1992) 877–887.
[4] S.J. Yeaman, The 2-oxo acid dehydrogenase complexes. Recent advances, Biochem. J. 257 (1989) 625–632.
[5] K. Nakano, S. Matuda, T. Yamanaka, H. Tsubouchi, S. Nakagawa, K. Titani, S. Ohta, Purification and molecular cloning of succinyltransferse of the rat α-ketoglutarate dehydrogenase complex. Absence of a sequence motif of the putative E3 and/or E1 binding site, J. Biol. Chem. 266 (1991) 19013–19017.
[6] K. Nakano, S. Matuda, T. Sakamoto, C. Takase, S. Nakagawa, S. Ohta, T. Ariyama, J. Inazawa, T. Abe, T. Miyata, Human dihydrolipoamide succinyltransferase. cDNA cloning and localization on chromosome 14q24.2-q24.3, Biochim. Biophys. Acta 1216 (1993) 360–368.
[7] K. Nakano, C. Takase, T. Sakamoto, S. Nakagawa, J. Inazawa, S. Ohta, S. Matuda, Isolation, characterization and structural organization of the gene and pseudogene for the dihydrolipoamide succinyltransferase component of the human 2-oxoglutarate dehydrogenase complex, Eur. J. Biochem. 224 (1994) 179–189.
[8] K. Nakano, M. Tanabe, S. Nakagawa, S. Ohta, S. Suzuki, M. Shimura, M. Matuda, Isolation and sequence analysis of the rat dihydrolipoamide succinyltransferase gene, DNA Sequence 13 (2002) 363–367.
[9] S. Matuda, J. Kodama, N. Goshi, C. Takase, K. Nakano, S. Nakagawa, S. Ohta, A polypeptide derived from mitochondrial dihydrolipoamide succinyltransferase is located on the plasma membrane in skeletal muscle, Biochem. Biophys. Res. Commun. 241 (1997) 151–156.
[10] Y. Yamabe, A. Shimamoto, M. Goto, J. Yokota, M. Sugawara, Y. Furuichi, Sp1-mediated transcription of the Werner helicase gene is modulated by Rb and p53, Mol. Cell. Biol. 18 (1998) 6191–6200.
[11] L. Wu, Y. Wu, B. Gathings, M. Wan, X. Li, W. Grizzle, Z. Liu, C. Lu, Z. Mao, X. Cao, Smad4 as a transcription corepressor for estrogen receptor, J. Biol. Chem. 278 (2003) 15192–15200.
[12] N. Frey, J.A. Richardson, E. N.Olson, Calsarcins, a novel family of sarcomeric calcineurin-binding proteins, Proc. Natl. Acad. Sci. U. S. A. 97 (2000) 14632–14637.
[13] F. Takada, D.L. Vander Woude, H.Q. Tong, T.G. Thompson, S.C. Watkins, L.M. Kunkel, A.H. Beggs, Myozenin: an α-actinin-and r-filamin-binding protein of skeletal muscle Z lines, Proc. Natl. Acad. Sci. U. S. A. 98 (2001) 1595–1600.
[14] T. Ikemoto, S. Komazaki, H. Takesima, M. Nishi, T. Noda, M. Iino, M. Endo, Functional and morphological features of skeletal muscle from mutant mice lacking both type 1 and type 3 ryanodine receptors, J. Physiol. 501 (1997) 305–312.
[15] G. Meissner, Ryanodine receptor/Ca^{2+} release channels and their regulation by endogenous effectors, Annu. Rev. Physiol. 56 (1994) 485–508.
[16] M. Kozak, Initiation of translation in prokaryotes and eukaryotes, Gene 234 (1999) 187–208.
[17] Y. Niimura, M. Terabe, T. Gojobori, K. Miura, Comparative analysis of the base biases at the gene terminal portions in seven eukaryote genomes, Nucleic Acids Res. 31 (2003) 5195–52013.
[18] Y. Xing, C. Lee, Evidence of functional selection pressure for alternative splicing events that accelerate evolution of protein subsequences, Proc. Natl. Acad. Sci. U. S. A. 102 (2005) 13526–13531.
[19] NCBI data bank for SNP: refer http://www.ncbi.nlm.nih.gov/snp.
[20] M.H. Stromer, Immunocytochemistry of the muscle cell cytoskeleton, Microsc. Res. Tech. 31 (1995) 95–105.
[21] G. Faulkner, G. Lanfranchi, G. Valle, Telethonin and other new proteins of the Z-disc of skeletal muscle, IUBMB Life 51 (2001) 275–282.
[22] N. Frey, E.N. Olson, Calsarcin-3, a novel skeletal muscle-specific member of the calsarcin family, interacts with multiple Z-disc protein, J. Biol. Chem. 277 (2002) 13998–14004.
[23] C. Faul, A. Dhume, A.D. Schecter, P. Mundel, A. Protein kinase, Ca^{2+}/calmodulin-dependent kinase II, and calcineurin regulate trafficking of myopodin between the Z-disc and the nucleus of cardiac myocytes, Mol. Cell. Biol. 27 (2007) 8215–8227.
[24] C. Etard, U. Roostalu, U. Straehle, Shuttling of the chaperones Unc45b and Hsp90a between the A band and Z line of the myofibril, J. Cell Biol. 180 (2008) 1163–1175.
[25] J.M. Sanger, J.W. Sanger, The dynamic Z bands of striated muscle cells, Sci. Signal. 1 (2008) pe37.
[26] T.D. Pollard, L. Blanchoin, R.D. Mullins, Molecular mechanisms controlling actin filament dynamics in nonmuscle cells, Annu. Rev. Biophys. Biomol. Struct. 29 (2000) 545–576.
[27] E. Nishida, S. Maekawa, H. Sakai, Cofilin, a protein in porcine brain that binds to actin filaments and inhibits their interactions with myosin and tropomyosin, Biochemistry 23 (1984) 5307–5313.
[28] H. Kuroyanagi, T. Kobayashi, S. Mitani, M. Hagiwara, Transgenic alternative splicing reporters reveal tissue-specific expression profiles and regulation mechanisms *in vivo*, Nature Methods 3 (2006) 909–915.
[29] B. Modrek, A. Resch, C. Grasso, C. Lee, Genome-wide detection of alternative splicing in expressed sequences of human genes, Nucleic Acids Res. 29 (2001) 2850–2859.
[30] B.J. Blencowe, Alternative splicing: new insights from global analyses, Cell 126 (2006) 37–47.
[31] J.M. Johnson, J. Castle, P. Garrett-Engele, Z. Kan, P.M. Loerch, C.D. Armour, R. Santos, E.E. Schadt, R. Stoughton, D.D. Shoemaker, Genome-wide survey of human alternative pre-mRNA splicing with exon junction microarrays, Science 302 (2003) 2141–2144.
[32] D.L. Black, Mechanisms of alternative pre-messenger RNA splicing, Annu. Rev. Biochem. 72 (2003) 291–336.
[33] T. Ohsako, T. Horiuchi, T. Matsuo, S. Komaya, T. Aigaki, *Drosophila lola* encodes a family of BTB-transcription regulators with highly variable C-terminal domains containing zinc finger motifs, Gene 311 (2003) 59–69.
[34] S. Kishore, S. Stamm, The snoRNA HBII-52 regulates alternative splicing of the serotonin receptor 2C, Science 311 (2006) 230–232.
[35] M. Hayakawa, E. Sakashita, E. Ueno, S. Tomonaga, T. Hamamoto, Y. Kagawa, H. Endo, Muscle-specific exonic splicing silencer for exon exclusion in human ATP synthase γ-subunit pre-mRNA, J. Biol. Chem. 277 (2002) 6974–6984.
[36] J. Tazi, N. Bakkour, S. Stamm, Alternative splicing and disease, Biochim. Biophys. Acta 1792 (2009) 14–26.
[37] M.J. Zylka, N.A. Sowa, B. Taylor-Blake, M.A. Twomey, A. Merrala, V. Voikar, P. Vihko, Prostatic acid phosphatase is an ectonucleotidase and suppresses pain by generating adenosine, Neuron 60 (2008) 111–122.